Hydrodynamic Analysis of a Surfboard

Vasco Dinis Henriques Breitenfeld
vascobreitenfeld@tecnico.ulisboa.pt

Instituto Superior Técnico, Universidade de Lisboa, Portugal

July 2024

Abstract

Even though surfing is a growing sport worldwide with a huge growth potential, it relies mostly on old techniques that incorporate its "soul and feel" for board design, rather than scientific data. The present work aims to develop a methodology to modernize the surfing industry through the introduction of Computational Fluid Dynamics (CFD). The tools used in this work include *Hexpress* for meshing, *ReFRESCO* as the CFD solver, and *Paraview* for post-processing. Firstly, a process to automate fin generation and mounting it to a surfboard was developed, using *Rhino* and *BoardCAD* to iterate on board and fin designs by generating CFD-ready CAD models with ease. Two sets of simulations were tested, the first including only the fins and the second a full surfboard model including the air-water interface (free surface). We found that the calculations on the fins present a simple, relatively fast way to generate a map of a fin layout's performance. On the other hand, surfboard calculations proved computationally costly, with lower quality results and more numerical instability due to the free surface modeling. While the boards' geometry did influence the fins' overall forces and coefficients, its inclusion was found to be too computationally demanding for industrial applications, presenting several unsolved issues with the Volume of Fluid(VOF) method. Knowing this, we suggest fin-only calculations are made, as they allow for easy comparison between multiple fin shapes and layouts, in a way that would be easily introduced in the industry without the surfboard calculations issues, complexity, and cost.
Keywords: Surfing, CFD, Fins, Free Surface

1. Introduction

Surfing, as one of the world's oldest sports, holds a prominent position in the recreational activities of numerous coastal regions. It involves a complex interaction between a surfer and its board to perform maneuvers and tricks. This study examines how the use of Computational Fluid Dynamics (CFD) in surfboard development could lead to performance enhancements.

Historically, surfboard evolution has been shaped by material and design innovations, with significant technological investments in recent decades. The first hollow board appeared in 1926, leading to a design revolution including the addition of fins for better stability and maneuverability [18]. Today's surfboards feature a foam core, a wide range of materials, and various shapes for enhanced performance.

Surfboard design has traditionally relied on intuition rather than scientific data. The present work proposes integrating CFD simulations into the design process, allowing virtual testing of surfboard models under various conditions.

This work will assess the practicality of full surfboard flow analysis in the industry and compare it to simpler fin-only calculations. The chosen CFD solver, *ReFRESCO*, offers specialized maritime features and employs the Volume of Fluid (VOF) method for fluid interaction modeling, namely the air-water interface.

Surfing's global popularity has turned it into a significant economic sector, with the market valued at €3.5 - €3.7 billion in 2022 and expected growth to €4.3 - €5 billion by 2027 [8, 20].

1.1. Current Surfing Development Model

Surfboard development traditionally involves a cycle between shapers and surfers. Shapers craft boards based on their expertise, while surfers provide feedback for improvements. This iterative process, enriched over time by technologies as Computer-Aided Design (CAD) and Computer Numerical Control (CNC), is based on the surfer-shaper relationship and is why surfing is considered to be based on "soul" and intuition [13].

1.2. Proposed Surfing Development Model

This thesis suggests adding a Numerical Optimization step to the development cycle, leveraging existing CAD models for simulations to identify and correct design flaws before boards and fins go into production. This step aims to enhance surfboard

performance and reduce prototype waste, potentially revolutionizing the design process and custom board creation for professional surfers. The compatibility with industry-standard tools and the potential for long-term benefits will underscore the value of this proposed model.

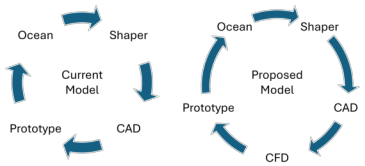

Figure 1: Current and Proposed Surfboard Design Processes.

2. Mathematical Models and Flow Solver

2.1. Governing Equations

The Navier-Stokes equations, consisting of coupled partial differential equations, describe fluid motion under various conditions. For incompressible fluids with a constant viscosity, with the continuity and momentum conservation equations found in equations (1) and (2) [2]. Continuity Equation:

$$\frac{\partial U_i}{\partial x_i} = 0 \tag{1}$$

Momentum Conservation Equation

$$\frac{DU_i}{Dt} \equiv \frac{\partial U_i}{\partial t} + U_j \frac{\partial U_i}{\partial x_j} = -\frac{1}{\rho}\frac{\partial p}{\partial x_i} + \nu \frac{\partial^2 U_i}{\partial x_j^2} + f_i \tag{2}$$

The Reynolds Averaged Navier Stokes equations (RANS) and Unsteady RANS (URANS) are used for modeling turbulent flows, decomposing quantities into (example: $\overline{u}$) and instantaneous components (example: u'), therefore for the case of the flow velocity: $U(x,t) = \overline{u}(x) + u'(x,t)$. [2, 14].

Continuity Equation:

$$\frac{\partial \bar{u}_i}{\partial x_i} = 0 \tag{3}$$

Momentum Conservation Equation:

$$_j \frac{\partial \bar{u}_i}{\partial x_j} = \overline{f}_i + \frac{\partial}{\partial x_j}\left[-\frac{1}{\rho}\overline{p}\delta_{ij} + \nu\left(\frac{\partial \bar{u}_i}{\partial x_j} + \frac{\partial \bar{u}_j}{\partial x_i}\right) - \overline{u_i' u_j'}\right] \tag{4}$$

2.2. Free Surface Modeling - Volume of Fluid Method

The VOF method models non-mixable fluid interactions by assigning a scalar volume fraction (α) to each cell, varying between 0 (water) and 1 (air)[14]. The solution will then compute the density and viscosity under the assumption of a homogeneous mixture, for a mixture of n species, in this case $n = 2$ for air and water [14].

$$\rho = \sum_{i_p=1}^{n_p} \rho_i \alpha_i \leftrightarrow \alpha\rho_{air} + (1-\alpha)\rho_{water} \tag{5}$$

$$\mu = \sum_{i_p=1}^{n_p} \mu_i \alpha_i \leftrightarrow \alpha\mu_{air} + (1-\alpha)\mu_{water} \tag{6}$$

$$\alpha = \frac{V_{air}}{V_{air} + V_{water}} \tag{7}$$

The method computes density and viscosity as a homogeneous mixture and introduces the scalar in the transport equation:

$$\frac{\partial \alpha}{\partial t} + \nabla \cdot (\alpha V_i) = 0 \tag{8}$$

Operational challenges include meeting the Courant–Friedrichs–Lewy (CFL) condition and ensuring uniform mesh refinement at the free surface height. The VOF requires the value of α to be kept between 0 and 1 to ensure the result is physically accurate, which is the main factor that affects convergence when it is used.

2.3. Turbulence Model - $k-\omega$ SST

The $k-\omega$ SST model, combining $k-\omega$ and $k-\varepsilon$ models, uses a function based on wall distance for smooth blending between models. It is widely used in hydrodynamics research and commercial applications for its effectiveness in simulating vortex development and free surface flows. As can be verified by the work of S. Qu *et al.* [16], the $k-\omega$ SST was found to be the most accurate model when modeling the free-surface interaction of a wave with another object (using a static cylinder) which is a good benchmark case for the present study where the free surface interacts with a static surfboard.

2.4. ReFRESCO Solver

ReFRESCO, developed by *MARIN*, is a CFD solver that uses the finite volume method, it is also compatible with various mesh types and post-processing tools. It features tools specially crafted for the maritime industry, such as advanced free surface modeling, crucial for maritime applications, and offers parallelization via *MPI*. Accessible on Linux, it supports *Hexpress* and CGNS meshes, with an intuitive *controls.xml* for the management of numerical settings.

2.5. Numerical Settings

Simulations used *ReFRESCO* version 2.9.0, targeting convergence with stable forces over 1000 iterations and residuals of L_2 norm at $5 \cdot 10^{-5}$ and L_∞ norm at $3 \cdot 10^{-2}$. Second-order time discretization and consistent time steps were ensured by a target Courant Number setting, meeting the CFL condition of the Courant number in the Free-surface section being ≤ 1.

All equations employed *MARIN* solvers for optimized performance. The momentum equation used the *MARIN GMRES* solver with *IMPLICIT-EXPLICIT* relaxation factors of 0.95 and 0.4, respectively. The pressure equation, using only explicit relaxation of 0.2, and the turbulence equation,

with eddy relaxation at 0.4, both utilized the same solver.

The free surface equation applied the *MARIN GMRESpol* solver and the *REFRICS* scheme for interface capture, with its explicit relaxation being set at 75% of the other equations.

3. Surfboard Types and Characteristics

Surfboards vary in design, tailored for specific surfing styles and waves.

- **Shortboards:** Highly maneuverable, around 1.82m (6 feet), with a pointed nose and tail for tricks and turns.
- **Longboards:** Stable and beginner-friendly, around 2.4m (8 feet), with rounded nose and tail for easy wave catching.
- **Funboards:** Balance of maneuverability and stability, around 2.1m (7 feet), with rounded nose and slightly pointed tail.
- **Fishboards:** For small to medium waves, known for speed, with a "V"-shaped tail and flat bottom.
- **Gunboards:** For big waves, most stable, typically over 2.4m (8 feet), with a pointed nose and wide tail.

3.1. Key Surfboard Features

- **Nose:** Rounded for stability (longboards) or pointed for control (shortboards).
- **Rocker:** Board curvature affects stability and maneuverability.
- **Tail:** Various shapes for different wave conditions and maneuvers.
- **Rail:** Side profile determining wave grip and turn dynamics.
- **Bottom:** Guides water flow, with five main profiles: flat, concave, double concave, convex, and Vee.
- **Outline:** Shapes connection impacting board performance, with parallel, curved, and hybrid outlines.

4. Surfboard Fin Dynamics

Fins enhance surfboard stability and maneuverability, introducing a pivot point for turns. Design factors include size, profile, and layout.

4.0.1 Fin Size

Fin size affects stability and speed. Larger fins increase lift and stability but add drag. Adjustments include:

- **Base Length:** Longer bases add stability but reduce maneuverability.
- **Depth:** Deeper fins improve stability at the cost of agility.
- **Rake:** Tilt Angle, affecting wave speed handling.
- **Toe:** The inward angle of fins, adjusted for performance.
- **Cant:** Top angle of fins, influences turns and stability.

4.0.2 Fin Profile

Fin shape, or profile, balances lift and drag.

- **Symmetrical Fins:** Center fins, even water flow, stable for long turns.
- **Flat Side Fins:** Halved symmetrical fins, lift at 0° angle, balance speed and control.
- **80/20 Fins:** Asymmetrical, higher drag, consistent across attack angles, better speed and maneuverability.

4.0.3 Fin Layout

Four main setups exist:

- **Single Fins:** Smooth, stable, less drag, ideal for long turns.
- **Twin Fins:** Speedy, maneuverable, challenging at high speeds, for small-medium waves.
- **Thruster Fins:** Three fins, stable, versatile, increased drag.
- **Quad Fins:** Twin and thruster benefits, stable, fast turns, suitable for large waves.

5. Studies on Surfboards

5.1. Fin Analysis

5.1.1 Optimization of Surfboard fins using CFD

Rana *et al.* [19] aimed to optimize fin design for the best lift-to-drag ratio using *CATIA V5*, *Ansys Fluent*, and *MATLAB*. The $k-\omega$ SST model was used with an inlet velocity of 10m/s ($Re = 9.98 \times 10^5$), focusing on a single fin at angles of attack from 0° to 24°. The optimization process yielded a fin design characterized by a high aspect ratio, medium sweep, and a symmetrical airfoil profile. The optimized fin design improved performance by 62% compared to the base design, with the maximum L/D ratio at 10° and stall point at 18°.

5.1.2 Analysis of the hydrodynamic performance of three and four-fin surfboards using computational fluid dynamics

Gudimetla *et al.* [10] investigated three and four fin surfboard configurations using *CFX*. The $k-\varepsilon$ and Reynolds stress turbulence models were used at various speeds (3, 5, 7, and 10m/s with $Re = 3.35 \times 10^5$,$Re = 5.59 \times 10^5$, $Re = 7.83 \times 10^5$, $Re = 1.12 \times 10^6$, respectively). The three-fin configuration showed maximum lift at a smaller angle of attack than the four-fin design (the magnitude of maximum lift was the same for both designs), suggesting it's more suitable for maneuverability, while the four-fin design is better for stability and speed.

5.1.3 Computational hydrodynamics of a typical 3-fin surfboard setup

Falk *et al.* [6] introduce a novel approach to fin simulations by employing a Computed Tomography (CT) scan of an existing three-finned board to obtain a realistic fin model. The $k-\omega$ SST model was used with URANS calculations at high angles of attack (above 20°).

The study calculated the lift and drag coefficients for the overall fin layout and for each fin, allowing for a better characterization of the system performance and showing the effects of the interaction of the wakes from the different fins

5.1.4 Numerical Investigation of the Hydrodynamics of Changing Fin Positions within a 4-Fin Surfboard Configuration

Falk *et al.* [7] compared two 4-finned quad configurations using the same parameters as their previous study, found in [6] including a switch from RANS to URANS at high angles of attack (AOA), at speeds of 5,7.5,10 and 18m/s ($Re = 6.21 \times 10^5$,$Re = 9.32 \times 10^5$, $Re = 1.23 \times 10^6$, $Re = 2.23 \times 10^6$, respectively).

The optimal setup for the 4-finned board was found and it was determined that the 4-finned board produces more lift than the 3-finned board (meaning the rider will have more stability but must make more force to turn) but also sees a significant increase in drag, which will reduce the boards' top speed.

5.1.5 Numerical Investigation of the Hydrodynamic Characteristics of 3-Fin Surfboard Configurations

Crameri *et al.* [4] explored lift and drag coefficients in a 3-finned thruster, using the $k-\omega$ *SST* model, similar to Falk *et al.* [7], but with RANS for all angles (0° to 45°), unlike Falk's URANS for AOA$\geq$ 20°. The L_2 residual target was $1 \cdot 10^{-3}$, higher than those recommended by *ReFRESCO* [17], likely due to computational limits, allowing RANS use across all angles despite flow separation effects. A dual-inlet, dual-outlet boundary condition was used. Fin design variations showed fin depth as the key performance factor, with URANS needed for further post-stall analysis.

5.2. Surfboard Pointing Forward

5.2.1 Hydrodynamic Characterization of Planing Surfboards Using CFD

D'Ambrosio's study [1] analyzed surfboard dynamics, not just fins, using *Star CCM+* to create an attitude matrix. Employing URANS and the $k-\omega$ *SST* model, with VOF for the air-water interface, the study varied surfboard tip height and angle of attack (0° to 12°) to assess performance impacts. The domain included a 13cm refinement zone at the 5m water level. Results detail lift, drag, moment, and center of pressure for surfboard performance comparison and design verification.

5.3. Maneuvering Surfboard Simulations

5.3.1 CFD for Surfboards: Comparison between Three Different Designs in Static and Maneuvering Conditions

Oggiano and Pierella [15] explored surfboard maneuvering dynamics without fins, using *Star CCM+* and URANS with the $k-\omega$ *SST* model. The VOF method modeled the air-water interface, focusing on angles of attack from 0° to 10°. The study analyzed lift, drag, and side forces on three surfboards at 4m/s and 8m/s, $Re = 2 \times 10^6$ and $Re = 4 \times 10^6$, respectively. This revealed the rocker's impact on lift and drag, but concluding the tail shape had little to no influence on these parameters.

6. Flow Analysis of Surfboard Fins

Surfboard fins significantly influence board behavior, affecting maneuverability, speed, and stability. This section outlines a methodology for isolated fin analysis using CFD, establishing a baseline for meshing and behavior analysis across multiple angles of attack. These results will then be compared to full-surfboard calculations to determine which has the best industrial implementation potential.

6.1. Fin Design Automation and Geometry Definition

An automated fin design tool was built as this was found to be a key step in reducing the difficulty associated with performing CFD simulations on surfboards and/or fins by automatically generating a CAD model ready to import to the meshing software. This tool was developed using *Grashopper*, a visual programming language for CAD software *Rhino*, which allows for the creation of a CAD model of a 3-finned thruster layout to be designed and tweaked.

6.1.1 Design Considerations

The program generates symmetrical center fins and mirrored side fins based on NACA 4-digit airfoils, facilitating comparison with existing literature [6, 7, 19]. Controls for fin parameters allow for quick design iterations.

The program automates symmetrical center and mirrored side fin generation using NACA 4-digit airfoils for easy comparison and rapid design iterations in *Hexpress*[21, 6, 7, 19]. A *Grasshopper* script constructs airfoil profiles, streamlining the CAD process without extensive knowledge. Users adjust fin parameters via sliders, including depth, rake angle, and span, with additional controls for toe and cant angles. The script ensures consistent fin geometry for streamlined CFD simulations.

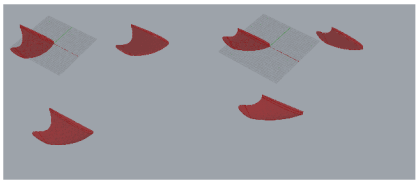

Figure 2: Two different fin systems created with the fin design tool.

The selected airfoil profiles for this study are the NACA 0006 and half-NACA 0012 for the central and side fins respectively. While the central fin is aligned with the direction of the surfboard it is going to be mounted in, each of the side fins has a

Table 1: Parameters used for the current fin layout.

Parameter	Value
Rake Angle	33.7°
Fin Length X	100mm
Fin Length Y	110mm
Bulge A	1.5
Bulge B	0.314
Continuity	1
Fin Middle Separation Sweep	1mm
Outboard Fins Cant Angle	6°
Outboard Fins AOA	2.75°
Outboard Fins Separation	160mm
Outboard Fins Vertical Adjustment	−15mm
Outboard Fins Distance to Mid Fin	210mm
Center Fin Profile	NACA 0006
Outboard Fins Profile	Half NACA 0012

2.75° toe-in angle and a 6° cant angle in the outward direction. The fin base is 100mm long and their depth is 110mm.

6.1.2 Meshing Considerations

To enhance the mesh quality for CFD analysis using *Hexpress*, a 1mm extrusion was added to fin designs, mitigating issues with cell skewness and orthogonality in the trailing edge due to its 0 thickness geometry. This modification assures *ReFRESCO*'s mesh criteria are met: equiangular skewness below 0.9 and orthogonality above 10°. The adjustment is deemed non-intrusive to the results, considering manufacturing tolerances would likely result in a non-sharp trailing edge.

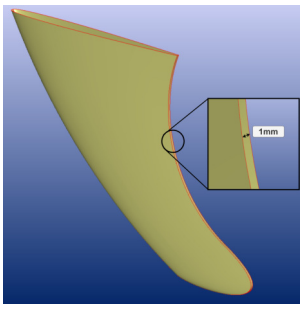

Figure 3: Center Fin Trailing Edge Adjustment.

6.2. Meshing

Hexpress was used to generate a domain for the fin layout, assuring *ReFRESCO's* quality standards were met (the equiangular skewness must not exceed 0.9 and the orthogonality must not be lower than 10°) and that the cell count remained within hardware limitations. The domain dimensions follow Crameri *et al.* [4] and Falk *et al.* [6], balancing the size and computational power (2.6m long in the flow direction (X-axis), with a width of 1m m (Y-axis), and a height of 0.7m (Z-axis). Surface refinements focus on the fins and their wake, with a Python script ensuring reliable mesh definition with parameters adjusted based on the angle of attack of the fins.

6.3. Refinement Zones

Key flow development zones around the fins were refined particularly their wake. The initial meshing included a refined cylinder around the fins and a rectangular zone across the domain. These were adequate for low angles of attack but insufficient for capturing unsteady phenomena at higher angles, necessitating increased mesh refinement in the wake region. Utilizing *Paraview*, wake angles were determined on a case-by-case basis, leading to the replacement of the cylindrical zones with three new arc-shaped zones for each fin, enhancing convergence and computational efficiency.

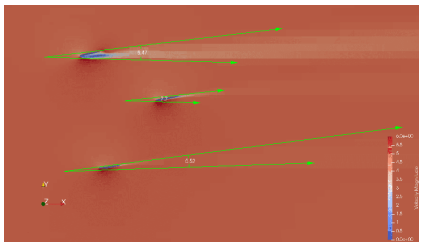

Figure 4: Wake Angle Measurements in *Paraview*.

6.4. Boundary Conditions

The top of the domain was designated as a "Free Slip Wall." The bottom surface of the domain was set as a "Symmetry Plane", and so were the left and right boundaries. The "Inlet" boundary condition was applied to the boundary nearest to the fins, with an inflow velocity of 5m/s in the X-axis. The outlet was set as a "Pressure Outlet" with a fixed pressure of 0Pa.

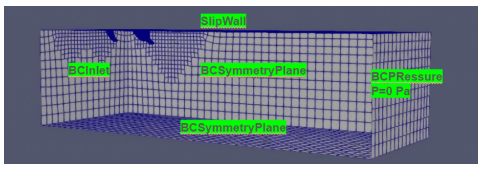

Figure 5: Boundary Conditions - fin-only case.

6.5. Numerical Setup

This study used *ReFRESCO v2.9.0* for all simulations. These were performed from 0° to 35° at 5° intervals. The $k-\omega$ SST turbulence model and a SEGREGATED algorithm were employed. For angles $\geq 10°$, unsteady calculations were necessary due to unsteady phenomena. Lift (C_L) and drag coefficients (C_D) were computed for comparison with board results and for the characterization of the fin layout. The reference area used to obtain these coefficients was 0.228m^2.

$$C_L = \frac{L}{\frac{1}{2}\rho v^2 A} \tag{9}$$

$$C_D = \frac{D}{\frac{1}{2}\rho v^2 A} \tag{10}$$

Table 2: Meshes for the uncertainty analysis study.

AOA (°)	Mesh	Elements	C_L	C_{D_P}	C_{D_f}
0	M4	1346954	-0.00006	0.00834	0.007438
0	M3	2564848	-0.00004	0.00683	0.007344
0	M2	7539023	-0.00012	0.00497	0.007286
0	M1	13174440	-0.00020	0.00401	0.007287
10	M4	1323571	-0.41532	0.06502	0.006893
10	M3	3407598	-0.40511	0.06030	0.007014
10	M2	8649798	-0.40123	0.05766	0.007156
10	M1	15842050	-0.39887	0.05625	0.007142

With ρ, the density being 999.1kg/m^3, and v, the flow velocity being 5m/s.

6.5.1 Prism Layers

Prism layers were placed on all fin surfaces to model boundary layer effects, with a targeted y^+ value of 0.1-0.5. The ideal prism layer thickness was iteratively determined to be 2.487×10^{-6}m.

6.6. Numerical Uncertainty

Reliability Analysis is a crucial step for ensuring reliable results in CFD simulations as highlighted by [5] and [12]. The focus is on Lift, C_L, and Drag coefficients, C_D, and their components, with convergence expected as grid refinement progresses. Simulations at 0° and 10° AOA align with the full surfboard model studies.

Table 2 details the meshes, showing convergence across refinements. Figures 6, 7 and 8 depict the uncertainty in C_{D_P}, C_{D_f}, and C_L, with most results within the acceptable uncertainty range for naval applications, except for C_{D_P} at 0° AOA. The verification confirms the robustness of the simulation process, from fin design to numerical settings, for subsequent analyses.

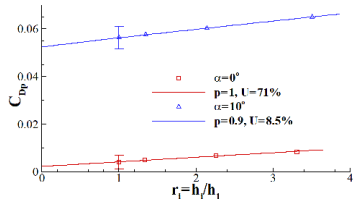

Figure 6: C_{D_P} uncertainty - 0° and 10° AOA.

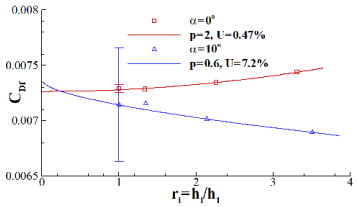

Figure 7: C_{D_f} uncertainty - 0° and 10° AOA.

7. Flow Analysis of a Full Surfboard Model Including Free Surface

7.1. Problem Definition

After fin behavior analysis, the study progresses to full board model calculations at various angles of attack. This introduces complex, computationally demanding calculations due to the board's interaction with the free surface. Boundary layer flow from the board's bottom surface is now considered, pointing to an expected impact on the fin performance. All calculations use URANS due to the unsteady nature of the generated waves, and the usage of the Volume of Fluid Method. The board, a Shortboard type with a 3-finned thruster setup, is placed in a 2m deep water domain under atmospheric conditions with a flow velocity of 5m/s.

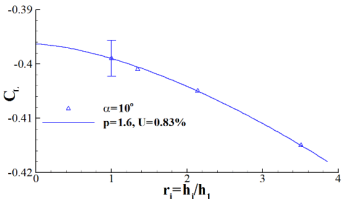

Figure 8: C_L uncertainty - 10° AOA.

7.2. Geometry Definition

The Shortboard, selected for this study, measures 1.82m by 0.468m by 0.138m, with fins mounted as per a real surfboard design. The Fin Design Automation software was updated to facilitate the board's positioning relative to the fins, allowing a board to be directly imported from *BoardCAD* as a *.step* file and create a single-bodied CAD model for CFD simulations or CNC production.

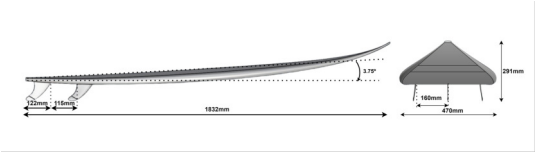

Figure 9: Dimensions of the Surfboard.

7.3. Meshing

The mesh, generated using *Hexpress*, is designed with domain dimensions based on the board's characteristic length. The domain extends 9.115m in length, with a 4m height to accommodate water and air flow development. A *Hexpress* script automates domain generation, refinement application, and board rotation for desired attack angles.

7.3.1 Volume of Fluid Method Considerations

The Volume of Fluid method captures the free surface behavior in surfboard simulations. Mesh cells within the free-surface section maintain equal Z-axis dimensions across the whole domain to reduce numerical diffusion due to hanging nodes[11]. The refinement zone encompasses the board's surfaces, requiring higher refinement due to the board's interaction with the water.

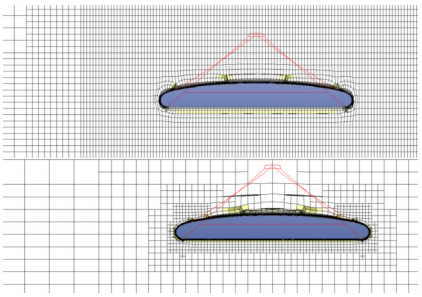

Figure 10: Top - Good Mesh without Hanging Nodes; Bottom - Bad Mesh with Hanging Nodes.

7.3.2 Geometric Considerations and Important Flow Regions

The surfboard geometry obtained from *BoardCAD* requires modifications for meshing. Key regions like rails, nose, and tail need specific refinement levels. The fins, divided into three surfaces like in the previous calculation set, have their refinement zone to accurately model their wake. This refinement zone is the same one used on the fin-only calculations.

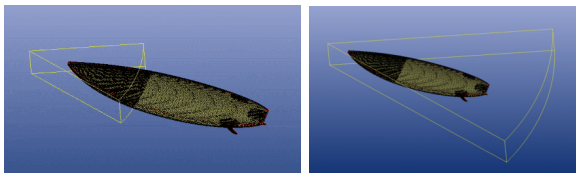

(a) (b)

Figure 11: Refinement zones around a) the surfboard nose and b) the surfboard body.

The Kelvin wake refinement zone starts 1m in front of the board, capturing the "V" shaped wake pattern.

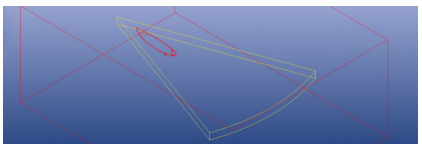

Figure 12: Refinement Zone - Kelvin Wake Region.

7.3.3 Computational Efficiency Refinement Zones

Strategies had to be found to increase computational efficiency due to limited resources and the added numerical complexity introduced by the FS zone. These included reducing the free surface zone's refinement zone height upstream of the board where water is expected to be calm and limiting refinement outside critical sections.

7.4. Numerical Setup

The reference length is the surfboard's length (L_{Board} = 1.823m), velocity is 5m/s (Re_{Board} = 6.14×10^6), and pressure is 0Pa, following *ReFRESCO* guidelines. Boundary conditions are set as per ITTC[3] and *ReFRESCO* recommendations[17] for Free-surface waves and vessels. The $k-\omega$ SST model is once more selected for its suitability in free-surface applications.

7.4.1 Boundary Conditions

The inlet was set as an "Inlet" with a velocity of 5m/s and the top of the domain as "Pressure" with a value of 0PA. The outlet was set as a simple "Outflow" whilst the left, right, and bottom were set as "Free Slip Wall".

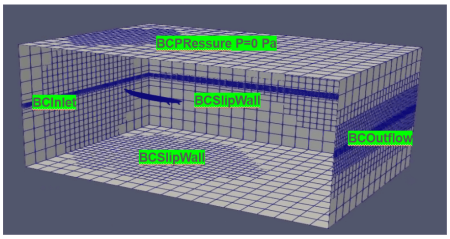

Figure 13: Boundary Conditions - Surfboard case.

7.4.2 Damping Regions

A damping region shaped as an ellipse with radii $2 \cdot L_{Board}$ and L_{Board} is implemented to prevent wave reflections from destabilizing the solution, allowing for accurate free surface development around the surfboard. This can be seen in Figure 14.

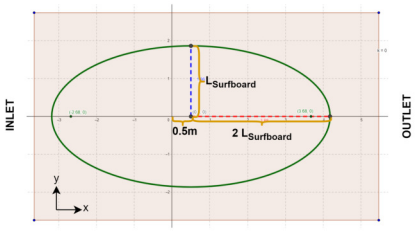

Figure 14: Damping Zone (Z = 2.05m).

7.4.3 Time Step

Time step selection adheres to the CFL criterion, with a target Courant number being kept considerably under 1 using iterative adjustment and monitoring in the early stages of the simulation to maintain stability and optimize computational efficiency.

7.5. Numerical Ventilation

This study encountered Numerical Ventilation (NV) on the surfboard's bottom surfaces, a common error in flow modeling around planning hulls, caused by air particles trapped in the boundary layer, leading to unrealistic flow patterns [9]. NV was evident when forces oscillated excessively. It was found that the surfboard's bottom was in contact with air, as shown in Figure 15. The surfboard's geometry, with rails instead of side walls

and a plane hull instead of a water-breaking hull, exacerbated NV, making the FS interaction zone crucial for accurate flow modeling around the rails.

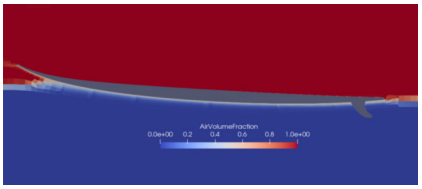

Figure 15: Calculation where NV problem was discovered (*contactLineCorrection* enabled, $y^+ = 50$).

Efforts to mitigate NV followed Gray-Stephens *et al.* [9], who suggested several solutions rated on effectiveness. Initial attempts included a modified High-Resolution Interface Capture (HRIC) Scheme named *REFRICS* in *ReFRESCO*'s case, refining the upstream free surface, and adjusting prism layer thickness, which increased mesh elements but did not resolve NV, as depicted in Figure 16.

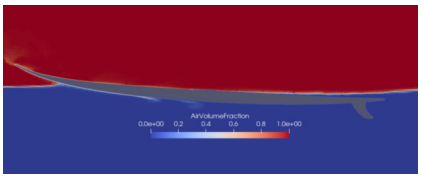

Figure 16: First Attempt at Fixing NV as suggested by [9] (*contactLineCorrection* enabled, $y^+ = 50$ on the interface contact zone, $y^+ = 1$ elsewhere).

Subsequent trials involved *contactLineCorrection*, a *ReFRESCO* setting designed to prevent NV by recalculating an air-to-water reaction on a given surface, yet NV persisted, as indicated in Figure 17. A breakthrough occurred with the usage of *BCSlipWallPressure*, a boundary condition allowing manual air-to-volume fraction input, which when applied to a critical board section, ensured water presence in the bottom surface and eliminated NV (Figure 18).

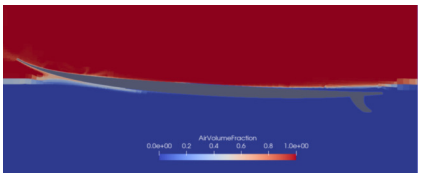

Figure 17: Second Attempt at Fixing NV as suggested by [9] (*contactLineCorrection* enabled, $y^+ = 1$ on the interface contact zone, $y^+ = 50$ elsewhere).

This solution improved convergence and wave patterns, despite introducing minor simulation errors due to the forceful value of α.

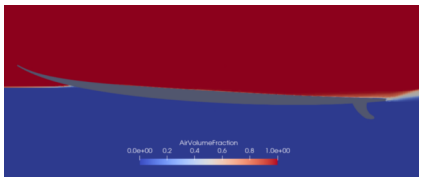

Figure 18: Final Solution - no Numerical Ventilation.

8. Results Analysis

8.1. Fin Analysis

After concluding the calculations for the fins at all angles of attack(AOA), the lift (C_L) and drag (C_D) coefficients could now be analyzed. It was found that maximum C_L occurred at a 20° AOA, with a peak lift-to-drag ratio at 5°. Beyond 20° the flow separates without reattachment on all 3 fins, causing pressure drag to increase and lift to decrease.

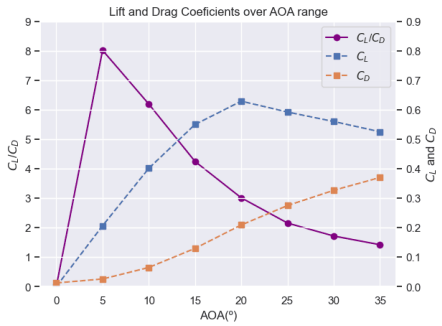

Figure 19: C_L, C_D, and C_L/C_D for the AOA range.

To visualize these phenomena, the total pressure surrounding the board was as shown in equation 11.

$$p_T = p + 0.5\rho(\sqrt{V_x^2 + V_y^2 + V_z^2})^2 \qquad (11)$$

And visualized across all AOA, in a region where the effects of the board boundary layer would not be affecting the fin if it was mounted on the board (Figure 20).

These comparative studies confirm the behavior in the C_L and C_D trends, as can be evidenced by the effects of viscosity. Mesh resolution impacted the fin's force generation, with coarser meshes overestimating lift and drag.

8.2. Analysis and Comparison of Board Results

The fin results were compared with full surfboard simulations to assess the board's influence. A coarser fin mesh was used for comparison due to computational constraints, affecting the detail and accuracy of separation regions and pressure gradients. This was the case as if a mesh that had the same number of elements per fin surface was used with the full surfboard case, computational times would be significantly higher, making this study impossible with the available resources. The coarsened

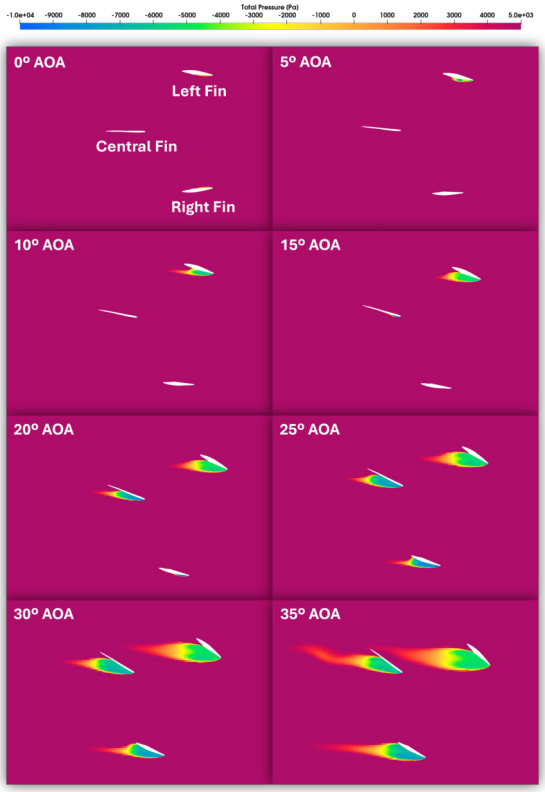

Figure 20: Total Pressure for all Angles of Attack [Pa].

fin mesh impact was isolated by comparing it with the finer mesh in fin-only simulations.

Board simulations, incorporating the VOF method, were limited to 0° and 10° AOA due to computational constraints. Higher AOAs presented challenges, particularly in areas where the free surface met the board's rail (Figure 21), concentrating the hard-to-capture free-surface effects on a single point.

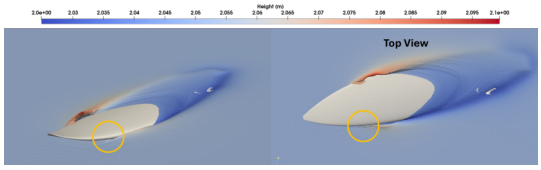

Figure 21: Problematic Area for $AOA \geq 10°$.

The boundary layer thickness approximation for turbulent boundary layers ($\delta \approx 0.37x/Re_x^{\frac{1}{5}} = 0.0227$m) and *Paraview* analysis determined the boundary layer's impact on the fins, affecting approximately 18% of the fin's height. Upon analyzing the results for C_L and C_D in the board calculation when compared to the fins, the reduction in lift and drag matches the portion of the fin that is directly affected by the boundary layer. Notably, the affected regions correspond to the wider portions of the airfoil, having a significant impact on the lift and drag forces generated by the fin (Table 3).

Table 3: C_L and C_D - Board and Fin Simulations.

Simulation	C_L	C_D
Board - 10°	0.314	0.060
Refined Fins - 10°	0.401	0.065
Coarse Fins - 10°	0.415	0.071

In the fin-only case, the boundary condition at the fin's top is a "Free Slip Wall," implying that the effects of the cantilevered section between the fin and the top surface are disregarded. Consequently, the fin behaves as though it is in isolation, effectively mirroring the top surface and, thus, effectively doubling its aspect ratio which increases its overall efficiency.

When the fin is mounted to the surfboard, the top surface is characterized by a "No Slip Wall" boundary condition. This condition entails that the wider top section of the fin ceases to generate lift as it did in the isolated scenario, resulting in a substantial reduction in the total lift produced by each fin. A comparison of both cases is presented in Figure 22.

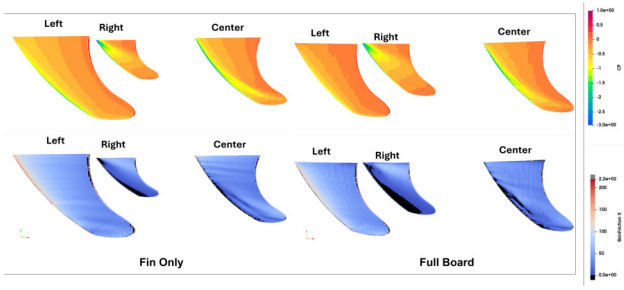

Figure 22: Comparison: Fin-only with full Board.

8.3. Computational Time Evaluation

This study evaluated the feasibility of full-scale surfboard simulations versus fin-only models, focusing on computational time. Simulations included steady-state fins, unsteady fins, and unsteady boards. Fin-only simulations were more time-efficient. All calculations were performed on a workstation with *Rocky Linux 8*, an *Intel Xeon CPU E5-2650 v2 @ 2.60GHz* with 16 cores, and 128GB of RAM. While full-board simulations offer comprehensive insights, they require significant computational resources, making them impractical for small to medium-sized manufacturers. Larger manufacturers might use fin-only simulations for performance profiling and reserve full-board models for high-level competitive scenarios.

Table 4: Comparison of Simulation Times.

Type	**Time (H)**	**Nº Simulations**	**Total Time (H)**
Steady State Fins	4.8	3	14.4 [0.6 Days]
Unsteady Fins	27.6	5	138 [5.75 Days]
Unsteady Board	168	2	336 [14 Days]

9. Conclusions

The present work explored the potential of CFD in surfboard and fin development, aiming to reduce reliance on physical prototypes. A gap in comparative studies between fin-only and full-surfboard simulations was identified, leading to an investigation into a process that could be implemented in the industry. A tool for automated fin design and board placement was developed, significantly streamlining the process of creating a CFD-ready CAD model.

Simulations on three fins in a thruster layout detailed their performance range, showing optimal efficiency at $0° - 20°$ AOA, with stalling observed beyond this range. These results were used to build a performance map for this layout.

The fin layout was tested on a full surfboard model, but only at $0°$ and $10°$ AOA due to computational limits and issues with the free surface. These results indicate lower C_L and C_D values compared to the fin-only model. These preliminary results suggest the influence of the board's bottom surface on fin performance, namely the difference between a cantilevered region in the full surfboard calculations compared the free slip wall in the fin calculations.

The study concluded that fin-only simulations are feasible for performance profiling in industrial applications or for individual shapers, while full-board models require further development, particularly for higher AOAs, and are not in a state where wider industrial application is recommended without significant computational resources.

10. Future Work

Future research should focus on overcoming free surface challenges at AOAs beyond $10°$ and exploring other mesh types for computational efficiency.

A comparison with a hybrid fin model, excluding the surfboard and free surface but including boundary layer effects, was considered. However, due to mesh resolution limitations, convergence was not reached. This model could offer a compromise between the fin-only and full surfboard simulations and improve the present work.

Collaboration with industry professionals such as shapers will also be key to integrating CFD into surfboard design, leveraging their insights to refine board design and align with market needs.

References

[1] Hydrodynamic Characterization of Planing Surfboards Using CFD. In *ISEA 2020*.

[2] V. d. Brederode. *Aerodinâmica Incompressível: Fundamentos*. IST PRESS, Lisboa, Portugal, 2014.

[3] I. T. T. Conference. Recommended procedures and guidelines 75-03-02-03: Preparation and conduct of towing tank test programs. *ITTC Proceedings*, 2023:1–100, 2023.

[4] S. Crameri, P. K. Collins, and S. Gharaie. Numerical investigation of the hydrodynamic characteristics of 3-fin surfboard configurations. *Applied Sciences*, 12(7):3297, Mar. 2022.

[5] L. Eça, M. Hoekstra, and G. Vaz. Verification of solutions in unsteady flows. ASME 2015 Verification and Validation Symposium, 2015.

[6] S. Falk, S. Kniesburges, R. Janka, R. Grosso, S. Becker, M. Semmler, and M. Döllinger. Computational hydrodynamics of a typical 3-fin surfboard setup. *Journal of Fluids and Structures*, 90:297–314, Oct. 2019.

[7] S. Falk, S. Kniesburges, R. Janka, T. O'Keefe, R. Grosso, and M. Döllinger. Numerical Investigation of the Hydrodynamics of Changing Fin Positions within a 4-Fin Surfboard Configuration. *Applied Sciences*, 10(3):816, Jan. 2020.

[8] Y. Finance. Global surfing market to reach $5.8 billion by 2027, 2022.

[9] A. Gray-Stephens, T. Tezdogan, and S. Day. Minimising numerical ventilation in CFD simulations of high-speed planing.

[10] P. Gudimetla, N. Kelson, and B. El-Atm. Analysis of the hydrodynamic performance of three- and four-fin surfboards using Computational Fluid Dynamics. *Australian Journal of Mechanical Engineering*, 7(1):61–67, Jan. 2009.

[11] C. W. Hirt and B. D. Nichols. Volume of fluid (VOF) method for the dynamics of free boundaries. *Journal of Computational Physics*, 39(2):201–225, 1979.

[12] C. M. Klaij, G. Vaz, and L. Eça. Numerical uncertainty estimation in maritime CFD applications. In *WCCM XI, ECCM V, ECFD VI*, Barcelona, Spain, 7 2014. International Association for Computational Mechanics.

[13] W. P. Magazine. How Computationer Fluid Dynamics and wave pools make magic sleds, 2022.

[14] MARIN. *REFRESCO Theory Manual*. Draft.

[15] L. Oggiano and F. Pierella. CFD for Surfboards: Comparison between Three Different Designs in Static and Maneuvering Conditions. In *ISEA 2019*, page 309. MDPI, Feb. 2018.

[16] S. Qu, S. Liu, and M. C. Ong. An evaluation of different RANS turbulence models for simulating breaking waves past a vertical cylinder. *Ocean Engineering*, 234:109195, Aug. 2021.

[17] ReFRESCO. *REFRESCO documentation - Tutorials*, March 24 2022. Report No.: ReFRESCO Tutorials, Version: 2.8.0.

[18] S. Roge. The heritage of surfboard design: Tom blake's hollow board, 1932, 2024.

[19] K. Sakellariou, Z. A. Rana, and K. W. Jenkins. Optimisation of the surfboard fin shape using Computational Fluid Dynamics and genetic algorithms. *IME, Part P: Journal of Sports Engineering and Technology*, 231(4):344–354, Dec. 2017.

[20] Statista. Surfing market size worldwide, 2022.

[21] S. Yoon. Naca airfoil generator, 2023.